EasyChair Preprint

№ 7736

A Novel Direct Ink Writing Manufacturing System to 3D Print Highly Concentrated Silk Fibroin

Enric Casanova-Batlle, Antonio J. Guerra and Joaquim Ciurana

April 8, 2022

Available online at www.sciencedirect.com

ScienceDirect

Procedia CIRP 00 (2021) 000–000

www.elsevier.com/locate/procedia

V CIRP Conference on Biomanufacturing

A novel direct ink writing manufacturing system to 3D print highly concentrated silk fibroin

Enric Casanova-Batlle[a], Antonio J. Guerra[b], Joaquim Ciurana[a]*

[a]*Grup de Recerca d'Enginyeria Producte Procès i Producció, Universitat de Girona*
[b]*EURECAT, Centre Tecnològic de Catalunya, Spain*

* Corresponding author. *E-mail address:* quim.ciurana@udg.edu

Abstract

Silk fibroin has demonstrated high biocompatibility in contact with the human tissue and in cell culture. As a result, it has been studied to develop very promising medical devices. The medical field has initiated a trend towards customization that will prevail in the recent future. That is why, 3D printed medical devices are gaining attention and becoming more relevant. This work attempts to unify silk fibroin with 3D printing. For this purpose, a high-concentration silk fibroin extrusion system has been designed. This system consists of a novel method to concentrate the fibroin to an optimal viscosity for direct ink writing. This could be accomplished due to the shear shinning property of the silk, after being expelled the viscosity keeps the shape of the silk in the place where it was deposited. Then, the system applies temperature to the silk to create a solid structure. A modular prototype has been created. It can print on any type of surface, flat or tubular. To evaluate the accuracy of the system on a flat printing bed, fluid flow rate and nozzle speed were evaluated in the fabrication of a mesh that simulated a flat cardiovascular stent. Images of the results were captured with a stereoscopic microscope, the dimensions of the result were calculated and compared with the chosen parameters. Thus, this work characterizes these features with the print resolution of the system. Finally, it opens a new paradigm for 3D printed medical devices based on silk fibroin.

Keywords: Type your keywords here, separated by semicolons ;

1. Introduction

Silk fibroin (SF) is a protein extracted from the silk cocoons of the *Bombyx mori* worm. It can usually be found in three different molecular structures, α-helix or random coil (silk I) and ß-sheet (silk II). Each of these structures has different properties [1]. These wide range on the features of the silk together with its biodegradability and biocompatibility has brought silk to gain importance in the field of biomedical devices. Silk has demonstrate safe effectivity in wound healing, applicability for bone regeneration, antibacterial activity, biosensors actuation, among others [2]–[4]. Typically in the past, silk-based products have been processed through sponges, films, gels, fibers, microspheres, etc [5]. However, these processes limit the morphology of potential SF products to the specific range of applications that can be manufactured. To expand the level of environments in which SF could be a valuable material, since it has the excellent mechanical properties, elicits minor immune responses, etc. A great efforts have been invested

* Corresponding author. *E-mail address:* quim.ciurana@udg.edu

in the implementation of SF in the additive manufacturing field. SF offers a key feature which makes 3D print feasible as a bioink, the shear thinning viscoelastic property [6]. Being able to 3D print SF, brings this material closer to applications that require less standard morphologies. Furthermore, it offers the possibility to be implemented for patient customization.

The implementation of the SF as an additive manufacturing asset has been attempted in the recent past. Three major 3D printing approaches have been experimented to fabricate medical devices with SF. Inkjet bioprinting has been used to 3D print SF as it allows a relatively cost-effective print with moderate printing speed [7]. Bone marrow stem cells were successfully cultured on a scaffold fabricated with inkjet SF printed lines [8]. Nevertheless, high concentrations of SF cannot be employed as it eludes nozzle clothing. Therefore, applications requiring more stable mechanical support are still under development. To avoid this hurdle digital light processing (DLP) has been employed to 3D print SF for tissue engineering purposes. This technique uses light, thus eliminating all the nozzle clothing problems. It manufactures the printed samples at high speed [9]. Nevertheless, it requires the addition of photo-crosslinking reagents to the bioink solution which complicates the ink formulation. Finally, the extrusion based system which was first described for SF by Ghosh *et al.* It was used to fabricate scaffolds to culture human bone marrow-derived mesenchymal stem cell which differentiated into chondrocytes. They concentrated the SF up to 28-30 wt % [10]. This blend was not viscous enough to maintain the deposited shape. That is why, the SF solution was deposited on a coagulation methanol reservoir. Printing without the coagulation step would significate to increase the SF concentration, thus the viscosity. However, a most common problem for the SF bioink is that when it is high-concentrated, it eludes to nozzle clotting [11]. The shear forces within the nozzle induce the gelation of the SF and its subsequent occlusion. That is why, efforts have been conducted to obtain recombinant silk to prevent this hurdle [11]. Basically, the recombined silk offers lower viscosity compared to native silk. Nevertheless, viscosity is highly recommended in this type of application because it ensures print fidelity. Precisely, low viscosity is a major problem of the low concentrated SF's bioinks. Moreover, applications where low-concentrated SF is used require binding the SF to additional additives. Collagen, glycerol, hydroxyapatite or gelatin are some of the typical materials which SF is often blended to fabricate extrusion SF 3D printing bioinks [12]–[14].

The innovative system presented in this study provides an alternative for printing highly concentrated SF with the extrusion method without the need to add additional reagents to the mixture and nozzle clothing issues. The gelation time of SF depends on many factors such as shear stress, temperature, concentration or pH. The approach taken in this study consists of increasing the pH of the dialysis solution to 8. According to the literature a concentration of 4 wt% at room temperature at pH 8 would take 50 days to gel [15]. The system presented in the paper has optimized the printing temperature of the nozzle, the temperature of the bed and the concentration of the solution to print high-concentrated SF avoiding nozzle clothing. As silk fibroin is aimed to be implemented for medical devices, a proof of concept study has been investigated for the fabrication of a cardiovascular stent with this technology. The study includes the optimization of the printing parameters in the stent features. A design of experiments (DOE) was performed to evaluate the effect of the printing flow and nozzle movement speed on the stent cell area (C_A) and stent strut width (S_W).

2. Methodology

2.1. 3D printing system

The 3D additive manufacturing machine developed for bioink printing was based on the 3-axis 3D printing technology. The concentrated SF solution was housed in a 5 mL discardit syringe (BD, United States) which was mounted on a supplementary support as depicted in Fig. 1. The SF ink traveled through a tube and was extruded through a precision G25 gauge needle (Nordson EFF, United States) that was mounted on the extruder. The ink was previously heated at 60 ºC in the gauge needle to enhance the formation of the β-sheet structures. This parameter was optimized to have the maximum temperature without clotting in the nozzle. As the evaporation of the water and the formation of more stable structures favour print fidelity. The bioink was pulled from the syringe to the needle between a flow ratio of 0.89-1.33 µL/mm by applying mechanical pressure on the top of the syringe. The ink was deposited on flat surface previously heated at 45 ºC at a speed range of 500 - 800 mm/min.

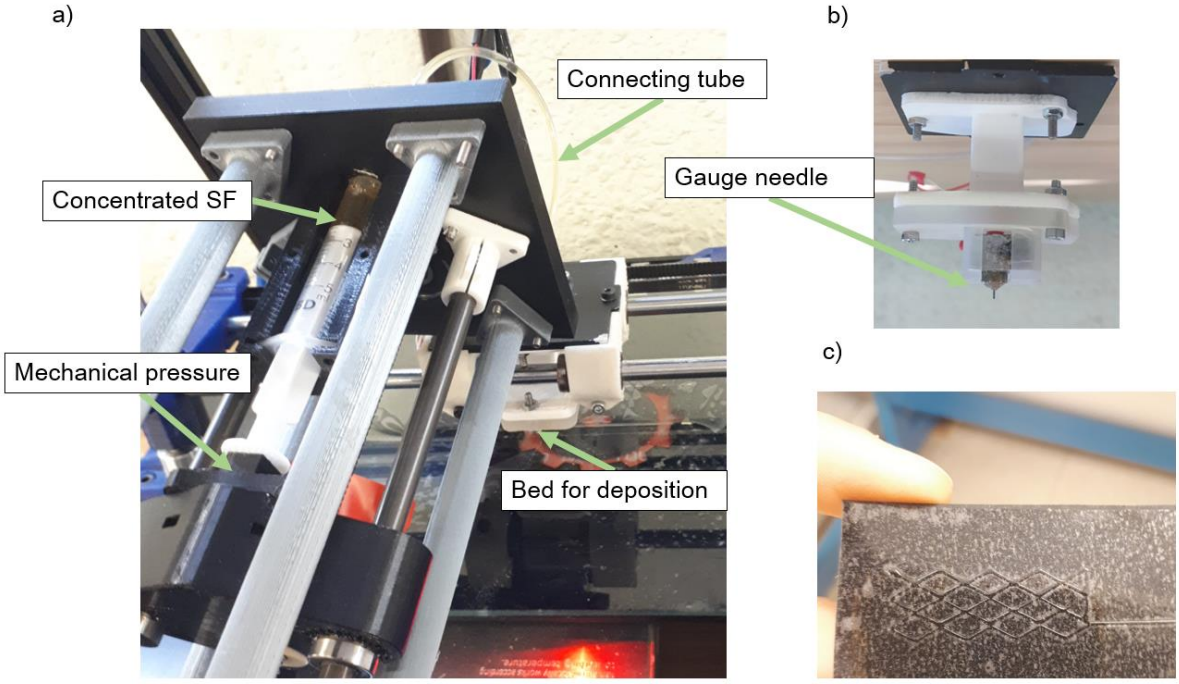

Figure 1 (a) SF extruder system. (b) Gauge needle inside the nozzle to control the extrusion temperature set up. (c) High-concentrated silk fibroin 3D printed cardiovascular stent.

2.2. Preparation of the bioink

Bombyx mori cocoons were kindly supplied by the association to preserve the silk worm in Spain (AERCEGSA) and the *Granja de la seda* institution for the development of the sericulture. Then, the SF was extracted according to the method previously described [5]. Briefly, to remove sericin from the silk, cocoons were immersed in 0.08 w/v% Na2CO3 (Sigma Aldrich) solution at boiling temperature for 30 min. Then washed with distilled water, and dried at room temperature overnight. The dried SF fibers were then dissolved in 9.3 M LiBr (Sigma Aldrich) solution and dialyzed against MiliQ water using a the SnakeSkinTM dialysis membrane of 3.5k MWCO for 2 days at 4 °C to remove the salt. The aqueous solution was then filtered with Miracloth (Milipore filter for gelatinous homogenates, Merck). The resulting SF solution was approximately 5 – 7 wt %. This aqueous solution was then dialyzed against 20 wt % PEG (8000 g/mol , Sigma Aldrich), 1M CaCl2 (Anhydrous > 93 %, Sigma Aldrich) and 50mM tris buffer (Sigma Aldrich) at 4 ºC using the SnakeSkinTM dialysis membrane of 3.5k MWCO. The solution was adjusted at pH =8. After 24 h the concentrated SF solution was 56.69 - 60.09 w/w %. It was removed from the dialysis membrane and stored at 4 °C before use. All the concentrations of SF were determined by comparing the weight of 0.5 mL of solution to the mass of silk after drying at 70°C for 12 hours.

2.3. Experimental design

The stent model used for the experiments was a diamond cell stent. The diamond side measured 5 mm, Fig. 1-c. A DOE was employed to relate the process parameters with the morphologic characteristics of the cardiovascular stent. The following process parameters were studied: fluid flow rate (F_R: 0.89-1.33 µL/mm), printing speed (P_S: 500/800 mm/min). The selected stent features analyzed were the stent C_A and the stent S_W. A Central composite design (CCD) DOE with 8 center points* and alpha 1.4142, (4 replicas). Therefore, 64 samples were printed.

Table 1.Design of experiments.

Parameter	Low level	High level
Printer speed (mm(min)	500	800
Fluid flow rate (µL/mm)	0.89	1.33

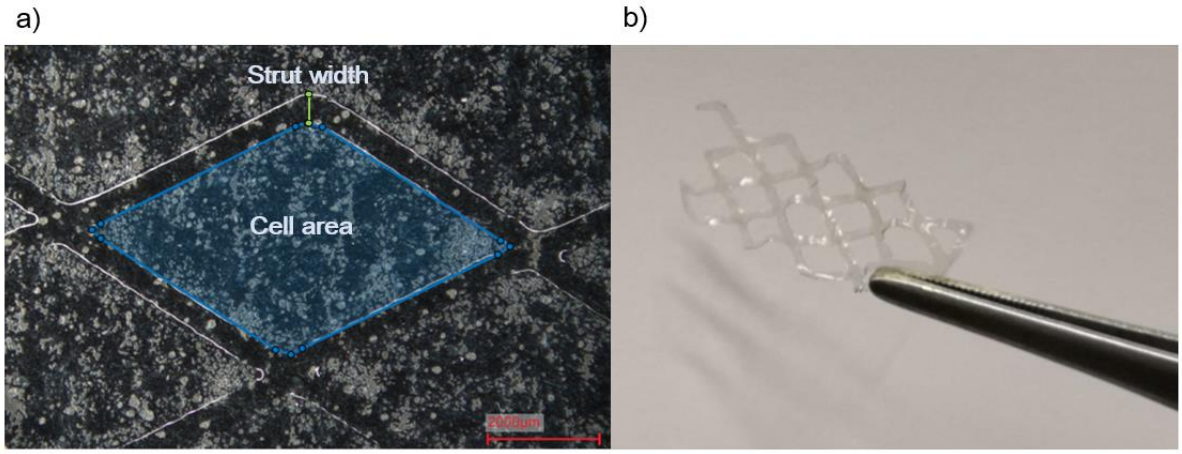

Figure 2 Stent geometry and parameters. a) Dimensional features. b) Example sample of a flat stent

2.4. *Characterization*

The dimensional characteristics (C_A and S_T) of each of the 64 samples were analyzed with a ZEISS discovery v12 stereo microscope coupled to the Invenio 20EIII microscope digital camera (5 Megapixel). Matlab® was used to process the images and collect the data. Three images of three different diamonds of the printed stent were randomly taken from each sample, Fig. 2. The average of these 3 values were represented in Fig. 3 and 4 (a-b).

3. Results

A linear regression model was calculated to fit the experimental data, eliminating the non-influential parameters ($p > 0.05$). A quadratic and polynomial model of degree 3 was also attempted. However, they did not present any influential variable in the results. The equation for the S_W parameter was described as follows:

$$S_W = +1.12 - 0.0014 * speed + 0.38 * flow \quad (1)$$

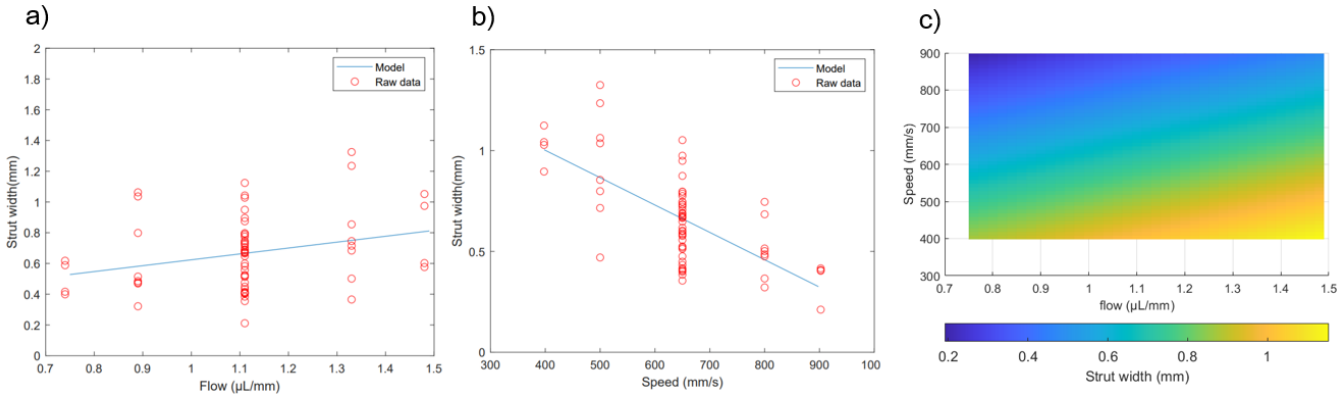

Figure 3 Fitted response plot of the regression model. The blue line represents the model found in the X-equation. It shows the response of the evaluated parameter in the studied range. The alternative parameter has been held constant at its mean value. The red markers indicate the experimental results plotted in their respective flow/speed value. (a) Depicts the S_w response for the flow rate variable. (b) Depicts the S_w response for the speed rate variable. (c) Surface plot of the interaction between the two variables with respect to S_W.

This indicates that both flow and speed are parameters that affect S_W. The lowest S_W during experimental data collection was 0.21 µm with the velocity at the high end and mean flow. However, according to Fig. 3-c there is a range of parameter combinations that could yield a resolution up to 0.2 µm. On the other hand, slower velocities with higher flows result in S_W thicknesses an order of magnitude higher. Being 1.32 µm the highest experimental value.

As expected these parameters have a complementary effect for the C_A parameter. Similarly a linear regression has been fitted

for the studied parameters and the A_C. Both parameters have been shown to have a significant influence on the value of this stent characteristic, Fig. 4.

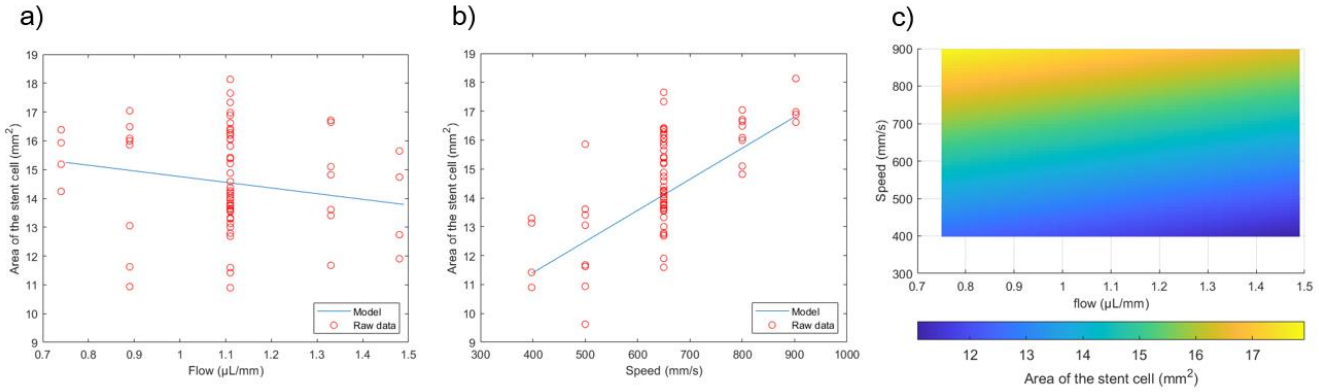

Figure 4 Fitted response plot of the regression model. The blue line represents the model found in the X-equation. It shows the response of the evaluated parameter in the studied range. The alternative parameter has been held constant at its mean value. The red markers indicate the experimental results plotted in their respective flow/speed value. (a) Depicts the A_C response for the flow rate variable. (b) Depicts the A_C response for the speed rate variable. (c) Surface plot of the interaction between the two variables with respect to the A_C

Being the side of the rhombus of 5 mm and the obtuse angle of 120º the theoretical area that should have the diamond is 21.64 mm^2. As the thickness of the strut overlaps the theoretical area of the rhombus smaller areas were found, being the largest 18.13 mm^2. Finally, the equation relating C_A to the printing parameters was as follows:

$$C_A = +9.7178 + +0.011 * speed - 1.97 * flow \quad (2)$$

4. Discussion

The reported results show a linear relationship between flow variation and the morphological stent parameters of S_W and C_A. The printing speed has a greater impact on the fabrication stent characteristics in the studied range, since the product of the factor multiplying speed by the speed range gives a greater weight to the equation than its respective flow value for both equations. This factor can occur because an increase in flow is merely an increase in the pressure exerted by the mechanical piston. This factor is not directly related to the amount of extruded material, since SF is a viscoelastic material, it stores the mechanical force in the form of pressure inside the syringe. Moreover, as we work with a very small tip (G25), although it is true that the more pressure the more material extruded, the flow through such a small orifice hinders this relationship. Moreover, after the prints, a small amount of material came out of the extruder when returned to its starting point. For this reason, if the relationship between pressure exerted and flow rate is not as direct as expected, velocity gains weight in the stent characteristics, Eq. 1-2. Speed basically controls the time the material has to exit the nozzle and therefore the amount of material deposited.

In addition, as expected, the relationship between C_A and S_W is complementary, since the head trajectory is the same, as there is more material, more thickness, the C_A decreases. In any case, the C_A characteristic of the stents were not occluded in any sample. S_W was continuous throughout the fabricated stents. Therefore, the fabricated stents were considered acceptable. These stents are manufactured through additive manufacturing technologies on a flat surface and are therefore a small proof of concept. The concept has been validated, as the innovative bioink has been used to manufacture medical devices such as cardiovascular stents. However, stents printed with additive manufacturing technologies are usually printed on a tubular surface [16], [17]. Therefore, the next steps would be to evaluate the mechanical properties of high concentration SF printed with this technique. Finally, print the cardiovascular stent on a rotatin mandrel.

5. Conclusions

SF was evaluated to create added value to additive manufacturing field. This study presented a SF based bioink that can be extruded without the need for additional reagents and avoiding the issue of nozzle clotting. A proof of concept was presented to verify whether the printing of medical equipment such as cardiovascular stents was possible with the bioink produced. The study has not only succeeded in verifying the feat, but also provides useful data to control the parameters of flow and printing speed. In the presented system, velocity had a major impact on the morphological characteristics of the stent. It can be controlled to print stents up to 0.2 mm S_W. Therefore, it has been demonstrated the potential of the printing system. Nevertheless, there is still a long way to go as the mechanical properties of the resulting material should be assessed. Finally, the system should be adapted to tubular printing.

References

[1] L. D. Koh *et al.*, "Structures, mechanical properties and applications of silk fibroin materials," *Progress in Polymer Science*, vol. 46. Elsevier Ltd, pp. 86–110, 01-Jul-2015.

[2] W. Zhang *et al.*, "Silk Fibroin Biomaterial Shows Safe and Effective Wound Healing in Animal Models and a Randomized Controlled Clinical Trial," *Adv. Healthc. Mater.*, vol. 6, no. 10, p. 1700121, May 2017.

[3] P. Bhattacharjee *et al.*, "Silk scaffolds in bone tissue engineering: An overview," *Acta Biomater.*, vol. 63, pp. 1–17, Nov. 2017.

[4] C. S. Shivananda, B. L. Rao, A. Pasha, and Y. Sangappa, "Synthesis of Silver Nanoparticles Using Bombyxmori Silk Fibroin and Their Antibacterial Activity," *IOP Conf. Ser. Mater. Sci. Eng.*, vol. 149, no. 1, p. 012175, Sep. 2016.

[5] D. N. Rockwood, R. C. Preda, T. Yücel, X. Wang, M. L. Lovett, and D. L. Kaplan, "Materials fabrication from Bombyx mori silk fibroin," *Nat. Protoc.*, vol. 6, no. 10, pp. 1612–1631, Oct. 2011.

[6] A. Panwar and L. P. Tan, "Current Status of Bioinks for Micro-Extrusion-Based 3D Bioprinting," *Mol. 2016, Vol. 21, Page 685*, vol. 21, no. 6, p. 685, May 2016.

[7] S. H. Kim, D. Y. Kim, T. H. Lim, and C. H. Park, "Silk Fibroin Bioinks for Digital Light Processing (DLP) 3D Bioprinting," *Adv. Exp. Med. Biol.*, vol. 1249, pp. 53–66, 2020.

[8] S. Limem, P. Calvert, H. J. Kim, and D. L. Kaplan, "Differentiation of Bone Marrow Stem Cells on Inkjet Printed Silk Lines," *MRS Online Proc. Libr.*, vol. 950, pp. 38–41, 2006.

[9] S. H. Kim *et al.*, "Precisely printable and biocompatible silk fibroin bioink for digital light processing 3D printing," *Nat. Commun.*, vol. 9, no. 1, Dec. 2018.

[10] S. Ghosh, S. T. Parker, X. Wang, D. L. Kaplan, and J. A. Lewis, "Direct-Write Assembly of Microperiodic Silk Fibroin Scaffolds for Tissue Engineering Applications," *Adv. Funct. Mater.*, vol. 18, no. 13, pp. 1883–1889, Jul. 2008.

[11] E. Desimone, K. Schacht, T. Jungst, J. Groll, and T. Scheibel, "Biofabrication of 3D constructs: Fabrication technologies and spider silk proteins as bioinks," *Pure Appl. Chem.*, vol. 87, no. 8, pp. 737–749, Aug. 2015.

[12] S. Hong *et al.*, "3D Printing of Highly Stretchable and Tough Hydrogels into Complex, Cellularized Structures," *Adv. Mater.*, vol. 27, no. 27, pp. 4035–4040, Jul. 2015.

[13] L. Sun, S. T. Parker, D. Syoji, X. Wang, J. A. Lewis, and D. L. Kaplan, "Direct-write assembly of 3D silk/hydroxyapatite scaffolds for bone co-cultures," *Adv. Healthc. Mater.*, vol. 1, no. 6, pp. 729–735, 2012.

[14] M. J. Rodriguez, J. Brown, J. Giordano, S. J. Lin, F. G. Omenetto, and D. L. Kaplan, "Silk based bioinks for soft tissue reconstruction using 3-dimensional (3D) printing with in vitro and in vivo assessments," *Biomaterials*, vol. 117, pp. 105–115, Feb. 2017.

[15] U. J. Kim, J. Park, C. Li, H. J. Jin, R. Valluzzi, and D. L. Kaplan, "Structure and properties of silk hydrogels," *Biomacromolecules*, vol. 5, no. 3, pp. 786–792, May 2004.

[16] A. Guerra, A. Roca, and J. de Ciurana, "A novel 3D additive manufacturing machine to biodegradable stents," *Procedia Manuf.*, vol. 13, pp. 718–723, 2017.

[17] A. J. Guerra, P. Cano, M. Rabionet, T. Puig, and J. Ciurana, "3D-Printed PCL/PLA Composite Stents: Towards a New Solution to Cardiovascular Problems," *Mater. (Basel, Switzerland)*, vol. 11, no. 9, Sep. 2018.